

# Lyotropic System Potassium Laurate/1-Decanol/Water as a Carrier Medium for a Ferronematic Liquid Crystal: Phase Diagram Study

V. Berejnov and V. Cabuil

*Equipe Colloïdes Magnétiques, Laboratoire I2C,<sup>†</sup> Université Pierre et Marie Curie, Bâtiment F, case 74, 4 place Jussieu, 75252 Paris Cedex 05, France*

R. Perzynski\*

*Laboratoire MDH,<sup>†</sup> Université Pierre et Marie Curie, Tour 13, case 78, 4 place Jussieu, 75252 Paris Cedex 05, France*

Yu. Raikher

*Laboratory of Complex Fluids, Institute of Continuous Media Mechanics, Perm 614013, Russia*

*Received: April 17, 1998; In Final Form: June 16, 1998*

Synthesis of lyotropic mixtures of potassium laurate, 1-decanol, and water is presented, and the phase diagram of this ternary system is investigated in the vicinity of the nematic region. Several phases are identified and the corresponding concentration and temperature-induced phase transitions are studied. To prepare ferronematic liquid-crystalline samples, positively charged magnetic nanoparticles are introduced into the lyotropic matrix. Modifications of the phase behavior of the system induced by the particle incorporation are described.

## 1. Introduction

Hybrid colloids resulting from association of lyotropic systems with polymers,<sup>1,2</sup> fine particles,<sup>3–7</sup> or proteins<sup>8</sup> are nowadays becoming a subject of extensive research. The purpose for synthesizing such complex structures is to obtain lyotropic liquid crystals (nematics, smectics, hexagonal phases) with genuine smart properties. For example, incorporation of magnetic nanoparticles into lamellar structures enables their orientation in magnetic fields of small intensity.<sup>7</sup>

Actually, lyotropic nematic systems as themselves can respond only to rather strong ( $\sim$ several kilo-oersteds) magnetic fields. A well-known example of a field-induced orientational effect is the magnetic Frederiks transition.<sup>9</sup> Introduction of magnetic nanoparticles into lyotropic nematics in order to enhance the magneto-orientational response has been considered in some theoretical<sup>10,11</sup> and experimental works.<sup>12,13</sup> However, any attempt to interpret the observed behavior needs a detailed description concerning the morphology of the system, its phase diagram, orientational properties, etc. Are the particles agglomerated? Where particularly are they located in the mixture? The answers to those and alike questions are of crucial importance.

In refs 12 and 13 interesting results on introduction of magnetic nanoparticles into a lyotropic system were presented. However, the prepared mixture was not stable: the particles agglomerated and the emerging aggregates separated from the nematic matrix. In our paper<sup>14</sup> we proposed to synthesize ferronematic samples by admixing to the same lyotropic system hydrophilic magnetic nanoparticles of  $\gamma$ -Fe<sub>2</sub>O<sub>3</sub>. The essential advantage is that, due to their individual surface charges, such particles do not agglomerate in water. With the ferronematic liquid crystals, thus obtained, we observe an orientational (Frederiks-like) transition at low fields, as described in ref 15.

For the synthesis of the systems in question, the problem of prime importance is to obtain a compatible phase behavior of both colloidal components when mixed. The question is a tricky one, since the size of magnetic particles in ferrofluids is of the same order of magnitude as the size of the micelles, which are the elementary structure units of the lyotropic nematic. As a departure point, one may look at the components separately. The phase behavior of ionic colloidal dispersions of magnetic nanoparticles has been clarified considerably in the recent works.<sup>4–7</sup> Also, the phase properties of the system potassium laurate/1-decanol/water as itself have been described more than once.<sup>16–18</sup> However, despite dealing with nominally one and the same system, its reported phase diagrams sometimes deviate significantly from one another. This circumstance should not be that surprising: as emphasized by the authors of refs 17 and 18, the synthesis of mesogenic lyotropic samples is a delicate point. The main difficulty is concerned with the fact that potassium laurate is not a commercially available product and is always synthesized by the team using it.

The objective of the present paper is to give a precise description of the developed synthesis scheme and to characterize (i) the components of the ternary system before mixing, (ii) the way of mixing, and (iii) the lyotropic compositions themselves. For the latter, the phase diagram is investigated in great detail that enables us to localize the domain of the nematic orientational ordering, to determine its borders and identify the types of structure organization in the adjacent regions. As the nematic state is very sensitive to any composition or temperature changes, introduction of a new component—the magnetic particles—considerably affects the phase behavior of the system. In the final part we summarize how association of nanoparticles with the surfactant micelles influences both the existence of the nematic ordering and the stability of the magnetic colloid.

## 2. Experimental Section

**2.1. Synthesis of the Samples.** *2.1.1. Materials.* The basic components of the system are commercially available ingredi-

\* To whom correspondence should be addressed. Fax: +33 01 44 27 45 35.

<sup>†</sup> Associated with the Centre National de la Recherche Scientifique.

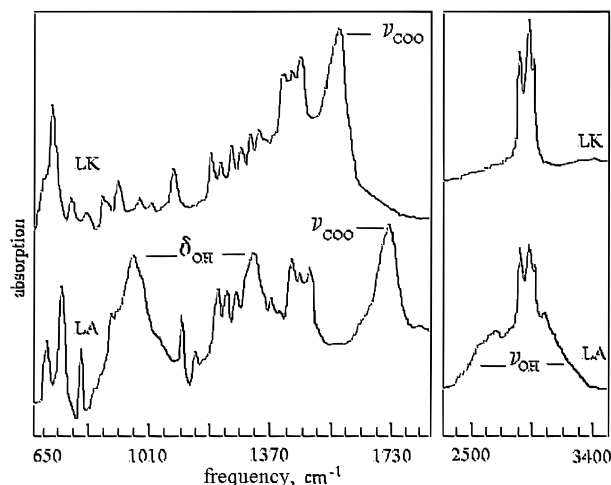


Figure 1. IR spectra of lauric acid (LA) and potassium laurate (LK).

ents, except potassium laurate, which has to be synthesized by alcalinization of lauric acid. In the latter procedure we use lauric acid (LA) purchased from Fluka (purity not less than 99%, indicated by manufacturer) as white solid platelets; potassium hydroxide (KOH) purchased from PROLABO (product content not less than 86%, total admixture of other alkaline metals not greater than 1%, indicated by manufacturer); this substance is a granular material. Ethanol was purchased from Fluka (product content not less than 99.9%, indicated by manufacturer). Water is distilled in the laboratory; its pH ranges between 5 and 6.

**2.1.2. Synthesis of Potassium Laurate.** Potassium laurate (LK) is obtained by alcalinization of lauric acid (LA) with KOH. Lauric acid is dissolved in ethanol at room temperature up to a concentration around 0.25 mol/L. The same volume of water is then added to the solution under vigorous stirring, and a concentrated aqueous solution of potassium hydroxide (9 mol/L) is added until the pH reaches 10.8–10.9. To the emerging highly viscous soap dispersion, six times its volume of water is added, and the diluted mixture is heated to the boiling point. Evaporation lasts until the total volume of the solution is reduced about 10 times against the initial one. Then water is added again, and evaporation is performed until the product is dry.

**2.1.3. Characterization of LK.** The obtained LK is a white powder, which dissolves in water at room temperature at concentrations up to 1 mol/L, the Kraft point being located at 5 °C. The pH of the aqueous 1 M solution is around 10.5 ± 0.2.

Purity of the precipitated LK, especially the absence of residual lauric acid, is verified using infrared spectroscopy (with a spectrometer UR-20). The spectra of LA and LK are compared in Figure 1. The main difference between them stems from replacement of the hydrogen atom by the potassium one in the neighborhood of the carboxyl group.<sup>19</sup> The disappearance of the bands 850–960, 1240–1300, and 2500–3400 cm<sup>-1</sup> and the shift of the band 1650–1725 to 1520 cm<sup>-1</sup> are the signature of the absence of LA.

We remark that the main subject of our investigation is the *ternary* lyotropic system and its phase diagram. That is why we try to eliminate the lauric acid as thoroughly as possible. Indeed, if present, it should be treated equally with the others as the fourth component, problem which falls far beyond the scope of the study discussed here. Having carried out numerous tests, we estimate the necessary level of purity of LK as LA ≤ 1 wt %. As soon as LK meets this condition, the phase diagram of the prepared lyotropic system prepared is reproducible in all its essential features. Yet another condition imposed on LK

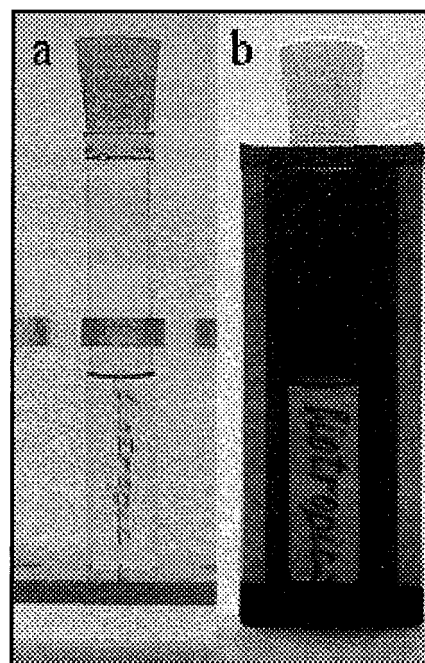


Figure 2. Lyotropic nematic sample: (a) the solution is clear and transparent; (b) between crossed polarizer and analyzer; the solution is birefringent.

and as well summarizing practical knowledge with regard to reproducibility is that the pH level of the product when dissolved in water at 20 °C must be inside the interval 10.3–10.7.

**2.1.4. Preparation of Lyotropic Mixtures.** First, we make at 90 °C a concentrated aqueous solution of LK (35 wt %, controlled by gravimetry), which is then cooled to 22 °C for further use. Thus, inhomogeneities due to possible ill dissolution of LK are avoided. The samples are prepared in laboratory tubes, which are opened when adding the components. This might cause evaporation and, consequently, modification of the composition. To keep track of these losses, the weight of each tube is regularly controlled. The LK aqueous solution is introduced first, and then 1-decanol is added drop by drop. Homogenization is performed, and the samples are centrifuged (still in the same tube, 2000 rpm, 2 min) in order to eliminate air bubbles. Thus obtained, the samples do not show any visual sign of changing over a period of at least six months.

**2.2. Methods to Study Phase States of a Lyotropic Sample.** **2.2.1. Samples.** The preparations are stored at constant temperature (accuracy ±1 °C) either in tightly closed cylindrical glass microtubes or in flat glass capillaries (from VITRO DYNAMIC, thickness 0.1 mm) used without any special surface treatment and closed at their ends by a transparent water-resisting lacquer. To get a point on the phase diagram, at least four identical samples of the same content are tested.

**2.2.2. Macroscopic Observations.** The macroscopic aspect (homogeneity, viscosity, and birefringence) of each sample is first checked by putting a tube in a cell formed by two crossed polaroids, see Figure 2. Contrary to thermotropic liquid crystals,<sup>9</sup> our lyotropic nematic samples are macroscopically homogeneous and transparent as clear water at thicknesses up to 1 cm. The pertinent estimations<sup>20</sup> of the cross-section for optical scattering yield it as 10<sup>-5</sup> of that for a thermotropic system. Their refractive indices are measured with a conventional Abbe refractometer.

**2.2.3. Microscopic Observations.** Microscopic crystallographic observations are performed at room temperature on the lyotropic samples put and sealed in flat glass capillaries

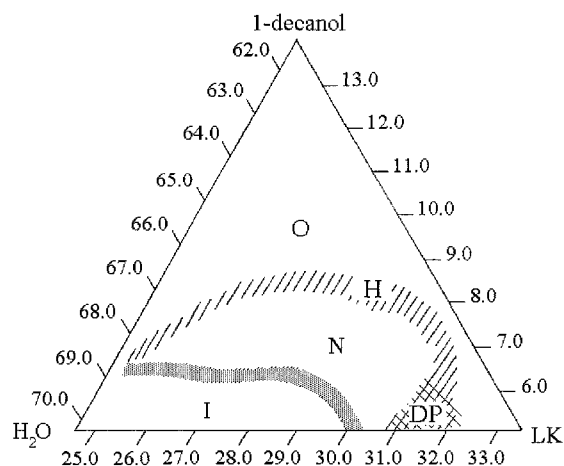


**Figure 3.** Ternary phase diagram of the system potassium laurate/1-decanol/water at 20 °C. Compositions are in weight percent; N stands for the nematic region, I for the isotropic, H, for the hexagonal, and O for the ordered phase. The DP region corresponds to the location of diphasic compositions. The gray area is the region into which pretransitional effects are observed.

(VITRO DYNAMIC) of thickness 0.1 mm. A POLAM R-11 microscope from LOMO is used both in the orthoscopic configuration to observe the structural defects and in the conosopic one to find the sign of optical anisotropy.<sup>21</sup> The latter is determined by the moving bands method with the aid of a quartz wedge KKK-3. A number of observations is done by putting under microscope the tubes themselves. The tube is tilted, and the solution inside forms a wedgelike layer with a free surface.

**2.3. Lyotropic Systems Doped with Magnetic Nanoparticles.** **2.3.1. Magnetic Particles.** Magnetic particles are made of maghemite ( $\gamma\text{-Fe}_2\text{O}_3$ ). We synthesize them by way of alcalinisation of aqueous mixtures of ferric and ferrous salts according to the procedure described in ref 22. The particle size distribution, as determined from magnetization measurements and small-angle neutron scattering,<sup>20</sup> is log-normal with the most probable diameter 7.5 nm and width 0.4. The particles bear surface charges due to the acid–base behavior of the ferric oxide surface. These charges can be modified through the pH of the medium in which the particles are embedded. We use here aqueous dispersions at pH 1–3, where nitric acid ensures the pH, counterions are nitrate anions. In these acidic solutions, the particles have positive surface charges and the colloidal stability is achieved owing to electrostatic repulsion.<sup>23</sup>

**2.3.2. Lyotropic Ferrodispersions.** The systems are prepared by admixing to the matrix an aqueous colloidal dispersion (usually called a *magnetic fluid*) containing about 3 vol % of ferrite nanoparticles. The actual compositions (at room temperature) are chosen according to the diagram of Figure 3, to be inside the nematic region but near the isotropic/nematic boundary. This choice is solely driven by practical considerations because in this region the systems are not too viscous. Having chosen the final composition, we prepare the lyotropic mixture with a precalculated deficiency of water. Then to this preparation the acidic magnetic fluid is added drop by drop under vigorous stirring. Together with the ferrite particles, it brings along the missing amount of water. In result, the point, representing the sample content in the ternary phase diagram, reaches the predestined position.

After having been doped, the compositions are cleaned by subjecting the samples to a magnetic field gradient ( $\sim 1$  T/m) for about 10 h. Normally, a certain amount of magnetic particles is excluded from the lyotropic solution. The magnetic grains

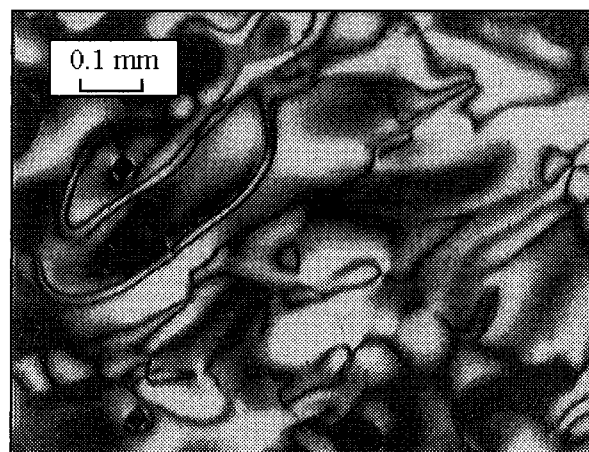


**Figure 4.** Typical microscopic observation of a sample in the N region, between crossed polarizer and analyzer.

settle in the high-field regions either as a magnetic precipitate or as a concentrated aqueous dispersion. This exclusion may turn out to be total, with no particles in the supernatant, or it is just partial. In the latter case, after removing aggregates, one obtains a homogeneous ferrolyotropic composition.

**2.3.3. Characterization of Lyotropic Ferrodispersions.** Concentration of the particles retained in the solution is measured by light absorption at  $\lambda = 480$  nm. Magnetization curves of the ferrolyotropic mixtures are recorded between 0 and 1 T with a Foner magnetometer<sup>23</sup> and compared to those of the ferrofluids used to dope the system. The orientational textures of the ferrolyotropic samples are tested with the same methods as used for the undoped ones.

### 3. Results

**3.1. Properties of the Undoped Lyotropic System.** **3.1.1. Structures Observed at Room Temperature.** Textures of the samples, observed between crossed polaroids, are characterized by their typical defects.<sup>24</sup> In the studied composition range (LK from 25 to 32 wt %, 1-decanol from 5 to 9 wt %, and water from 62 to 68 wt %), polarized-light microscopy at room temperature ( $T = 20$  °C) reveals a number of states. We identify the following:

(1) An isotropic phase (I), which is observed in the range  $\text{LK} < 30$  wt % and 1-decanol  $< 2$  wt %. The solution is a transparent fluid of low viscosity, optically isotropic.

(2) A nematic phase (N), which is observed for LK concentration between 25 and 32 wt % and that of 1-decanol ranging between 5 and 8 wt %. It is a clear solution with the viscosity about that of glycerol, optically anisotropic. In polarized light a texture characteristic of a nematic liquid crystal is observed (Figure 4).

(3) A very viscous phase, strongly birefringent, is observed for  $\text{LK} \sim 32$  wt % and 1-decanol  $> 8$  wt %. Its specific defects are shown in Figure 5. Since they strongly resemble those inherent to a hexagonal phase,<sup>25,26</sup> we denote this state as H. Note that its range of existence with respect to 1-decanol is rather narrow.

(4) An ordered phase (O), extremely viscous, is found at high concentrations of LK ( $> 33$  wt %) and 1-decanol ( $> 9$  wt %).

(5) A diphasic domain (DP) is located between the isotropic and nematic regions. It is characterized by a high dependency of its apparent viscosity on temperature and on the amount of alcohol. At 20 °C and for the composition indicated in Figure 6, it looks under polarization microscope as an emulsion of disc-shaped droplets, strongly birefringent, on an isotropic background.





**Figure 5.** Typical microscopic observation of a sample in the H region, between crossed polarizer and analyzer.

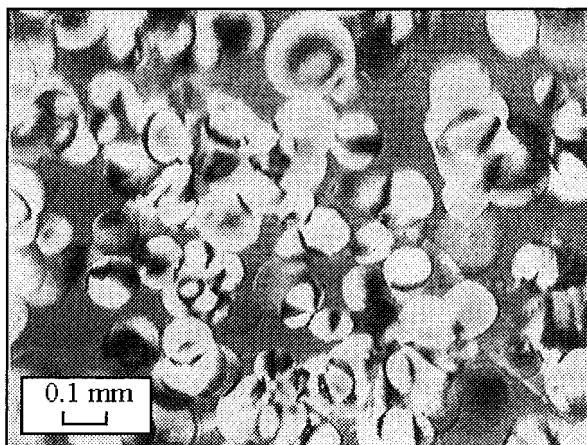


**Figure 6.** Typical microscopic observation of a sample in the DP region, between crossed polarizer and analyzer. Birefringent droplets are observed dispersed in an isotropic phase.

All these observations at 20 °C are summarized in the ternary diagram of Figure 3. To determine the boundaries of the nematic phase, more than 300 samples have been prepared, on the basis of different LK products. The results are always found to be reproducible.

**3.1.2. Phase Transformations with Temperature.** The succession of phases observed is summarized in Figure 7, which describes the ( $T$ , 1-decanol) phase diagrams for different compositions as characterized by the ratio water/LK. For all the compositions, there is a low-temperature range in which the transition  $I \rightarrow N$  takes place without any sign of a diphasic situation. This temperature range is wider the greater the ratio water/LK. In this range, pretransitional phenomena, reminiscent of the flicker effect,<sup>9,27</sup> are observed. Namely, when at low temperature, an isotropic solution that is sufficiently close to the  $I/N$  border (we conditionally denote this area as  $I_F$ ) readily responds to external perturbations by formation of macroscopic domains possessing optical anisotropy and presents giant orientational fluctuations. Actually, if the microtube is observed in a crossed-polaroid cell, any small vibration causes *bright flashes of light* against a black background. The intensity of the response grows strongly upon approaching the  $I/N$  border, no matter what concentration or temperature "route" is chosen. We remark that a similar effect was also encountered some time ago in the lyotropic system sodium decylsulfate/1-decanol/water.<sup>27</sup>

At higher temperatures, the transition clearly displays the features of a first-order one. In particular, the diphasic domain

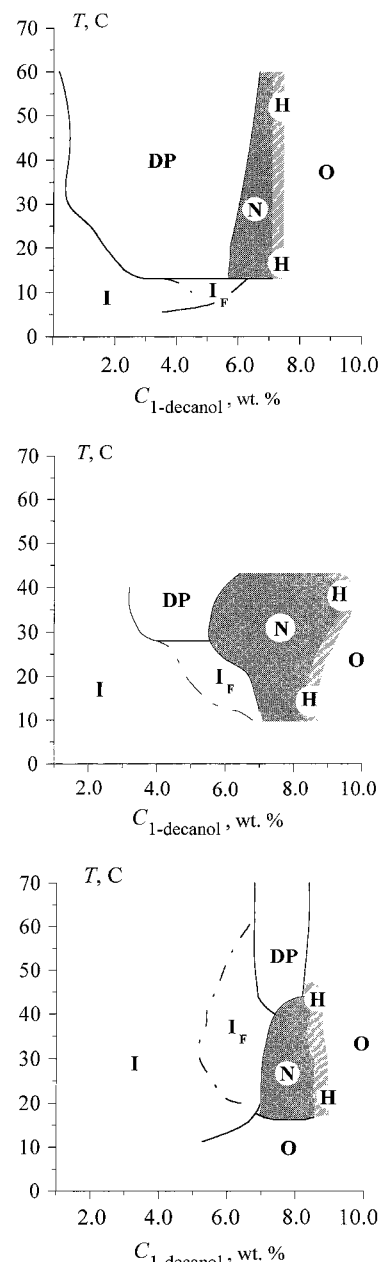


**Figure 7.** Phase diagrams  $T/1$ -decanol for the samples characterized by different values of the water/potassium laurate ratio: (a, top) 2.02, (b, middle) 2.28, (c, bottom) 2.51; here  $I_F$  denotes the region where pretransitional effects are observed.

is the more pronounced the lower the ratio water/LK. At room temperature, as Figure 7a shows, with the growth of the alcohol content the isotropic monophase gives up to a two-phase system, which appears as an emulsion of nematic microdroplets in an isotropic medium. Further on, the droplets grow in number and begin to unite, and then the emulsion "reverses" and the nematic monophase emerges. These transformations are accompanied by drastic changes of the rheology of the medium: its viscosity reaches a high maximum approximately halfway between  $I$  and  $N$ .

We remark that the  $I \rightarrow N$  transformation is reversible for any concentration or temperature "route" at the condition that the sample is kept not too long ( $<10$  min) under diphasic conditions. Then, the viscous DP state does not have enough time to develop itself.

As to the transformation  $N \rightarrow H$ , it begins with appearance of domains with a hexagonal-like ordering. Those domains

**TABLE 1: Compositions of the Samples Studied<sup>a</sup>**

sample	<i>T</i> (°C)	LK (wt %)	water (wt %)	1-decanol (wt %)
A	20–60 °C	25.2	69	5.8
B	20 °C	30.4	63.0	6.6
C	20 °C	28.0	64.8	7.2
C'	29 °C	28.7	64.6	6.7
D	20 °C	26.4	66.8	6.8
D'	22 °C	26.5	66.3	7.2

<sup>a</sup> Refractive index of sample A has been measured for different temperatures. Samples B, C, and D have been studied by conoscopy. Samples C' and D' have been characterized by orthoscopic observations.

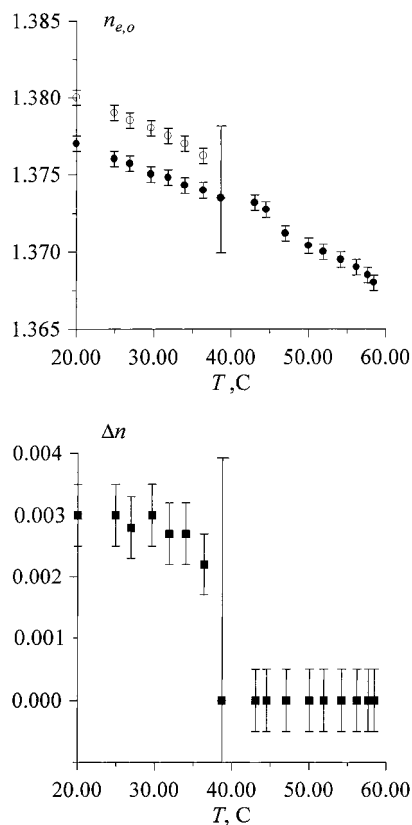


**Figure 8.** Variation of the refractive indices (a, top) and of the birefringence (b, bottom), for a sample of composition LK = 25.2 wt %, 1-decanol = 5.9 wt %, water = 68.0 wt %, as a function of temperature. For this sample the  $I \rightarrow N$  transition is observed at 40 °C.

grow with time and, finally, occupy all the available volume of the vessel. We do not detect any hysteresis, and the transition appears to be reversible.

**3.1.3. Characterization of the Nematic Phase.** The nematic phase is studied by (i) measurements of its refractive indices; (ii) orthoscopic observations between crossed polaroids to check the structure defects; (iii) conoscopy measurements to determine the sign of the optical anisotropy. In Table 1 the compositions of the tested samples together with the temperature of observation are indicated.

**Refractive Indices and Birefringence.** Figure 8a shows, for a sample characterized by a typical composition water = 69 wt %, LK = 25 wt %, 1-decanol = 6.0 wt % (sample A), the evolution of the refractive index of the lyotropic mixture with temperature. The same evolution is given for the birefringence in Figure 8b. The  $I \rightarrow N$  transition is clearly reflected in these figures. For all the nematic compositions we studied, the birefringence is always found to range between  $2 \times 10^{-3}$  and  $5 \times 10^{-3}$ .

**Structural Defects.** First, we note that the way in which capillaries are filled strongly influences observations. Filling

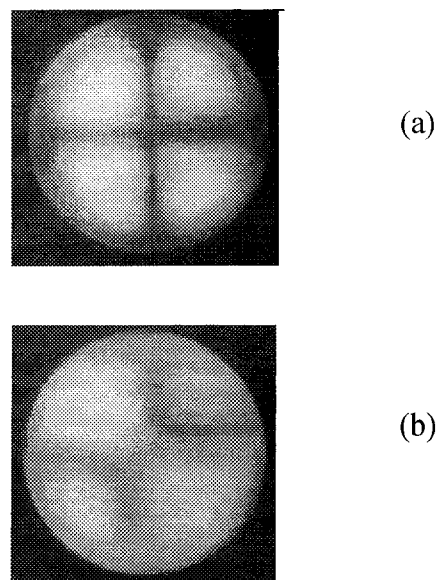


**Figure 9.** Conoscopic figures observed in capillaries filled with the lyotropic of the content C, see Table 1: (a) uniaxial pattern obtained when sampled under capillary forces; (b) biaxial pattern when sampled under vigorous stirring; this biaxial pattern is a transient one as illustrated by Figure 10.

very slowly, by the capillary forces, the number of defects is very small or they are visually absent. Oppositely, forcing the fluid during the sampling causes various defects that are the more numerous and long living the farther the representing point of the nematic composition from the  $I/N$  boundary.

Whatever the composition, the texture we observe at equilibrium, choosing the perfectly aligned areas of a sample, is always uniaxial. Two types of structural defect patterns can be encountered. They correspond to the director either perpendicular (homeotropic) or parallel (planar) to the cell walls, respectively. Typically, the nematic composition LK = 26.5 wt %, 1-decanol = 7.2 wt %, water = 66.3 wt % (sample D') at room temperature presents a homeotropic texture. In the lyotropic system under study the latter is associated with a discotic phase.<sup>24</sup> On the other hand, at higher temperature ( $T = 29$  °C), in sample C' we observe a planar configuration characteristic of a calamitic phase.<sup>24</sup>

**Conoscopy.** Conoscopic observations at 20 °C (samples B, C, and D) show that for perfectly oriented samples, corresponding to slowly filled capillaries, the uniaxial texture emerges all over the capillary as soon as the sample is prepared and does not evolve with time. For all the defectless sites of a capillary, a cross with concentric isochromates, corresponding to a uniaxial texture with positive optical anisotropy, is observed. The interference pattern is well-defined. The observed isogyre cross has an equal-wing form, and the pattern is completely stable against rotation around the optical axis (Figure 9a). The number of resolved isochromates, which determines the order of the observed interference (for the same tuning of the optical system), depends on the refraction index of the sample. For the studied solutions the maximal number of isochromates is two.

In general, conoscopic observations of the samples of Table 1 at  $T = 20$  °C yield their equilibrium texture as a discotic one with a uniaxial positive optical anisotropy.

**Transient Situations.** Orthoscopic observations show that as a result of a quick filling up, the liquid crystal becomes multidomain. Since those domains are of considerable size and long-living, we perform conoscopy measurements within the area of one domain. Definite but weak signs of biaxiality are

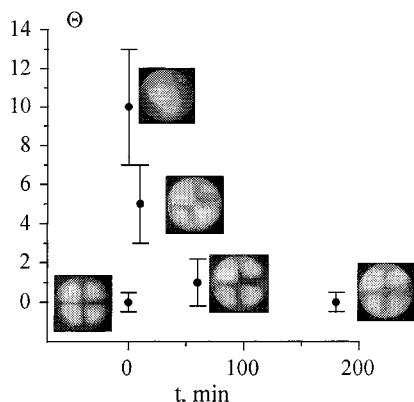


**Figure 10.** Evolution with the time of the conoscopic patterns for sample D. Here  $\theta$  is the experimental angle measuring the gap between the observed and uniaxial patterns. The leftmost pattern is the reference one, corresponding to the same lyotropic composition in equilibrium.

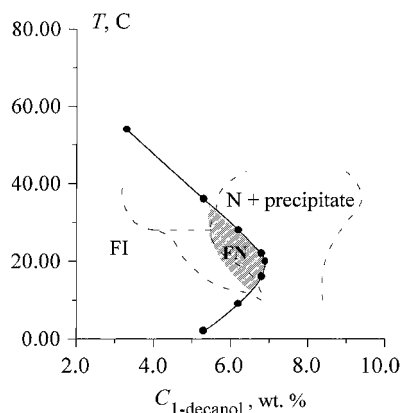


**Figure 11.** Diagram  $T/1$ -decanol for lyotropic samples doped by magnetic nanoparticles (volume fraction of particles being 0.06%). Shaded area corresponds to monophasic ferronematic samples. Dashed lines indicate the same diagram for the undoped system (Figure 7b). To the right of the solid line, particles are excluded from the lyotropic matrix.

observed. Visually, as the stage rotates, the cross pattern periodically falls apart into hyperbola branches with a very small interapex separation as shown in Figure 9b. This means that qualitatively the observed symmetry is biaxial, but with a rather small (of the order of  $10^{-4}$ ) refraction anisotropy  $\Delta n$ . However, the observed biaxial patterns seem to exist just in nonequilibrium situations since with the time the sample inevitably restores its uniaxial symmetry. The settling time (which may range from a few minutes to several days) turns out to solely depend on the location of the representing point of the solution on the concentration phase diagram. At a given temperature, this time is the longer the farther is the given point from the I/N boundary along the line of a constant 1-decanol concentration. Figure 10 compares the conoscopic patterns of sample D for slowly and quickly filled capillaries. The leftmost experimental point corresponds to the sample created in a quasi-equilibrium way. The cross is well-defined and does not evolve with time. The other points render the time evolution of the same nematic but sampled rapidly. Just after the filling is finished (the point  $t = 0$  at the time axis), the conoscopic cross is ill-defined, but as the equilibrium situation is recovered, it becomes distinct and clear. The reference relaxation time for the biaxial conoscopic patterns of Figure 10 is around 5 min.

**3.2. Properties of the Magnetically Doped System.** **3.2.1. Phase Diagram.** Figure 11 compares the diagram ( $T/1$ -decanol) of the undoped system (dashed lines, from Figure 7b) to that of the doped system, at the highest particle concentration (0.06

vol %) that we investigated systematically. The plotted data show the existence range of a stable monophasic ferronematic (shaded area).

The diagram of Figure 11 shows that the ferronematic region is considerably shrunk with respect to that of the pure system. The position of the I/N transition (now, FI/FN) remains practically unchanged. In some interval, as the concentration of 1-decanol increases, we observe a homogeneous ferronematic system. However, this interval is limited. Upon reaching a temperature-dependent threshold in 1-decanol, the magnetic particles are expelled. A diphasic situation occurs, where a precipitate of particles coexists either with a pure nematic liquid crystal or with a ferronematic whose particle volume fraction is reduced.

We remark that the phase behavior at the FI/FN border differs qualitatively from that for a pure system. The diphasic region (cf. Figures 7 and 11) disappears, and with the accuracy of our observation the transition looks as a second-order one. It is accompanied by a noticeable pretransitional light scattering due to refraction index fluctuations.

**3.2.2. Magnetic Properties.** Magnetization curves of the lyotropic ferrodispersions obtained in cells of thickness of a few millimeters are the same as those of magnetic fluids of same particle volume fraction. This is in favor of the fact that the particles are individually dispersed in the lyotropic matrix. This point is confirmed by our recent SANS experiments.<sup>20,28</sup>

The equilibrium orientational texture of our lyotropic ferrodispersions tested by polarization microscopy of structural defects in microcapillaries is always found to be uniaxial. As in the undoped system, two typical patterns are encountered. A homeotropic configuration corresponding to a discotic (now, ferrodiscotic) sample is observed at room temperature for the system of the content LK = 26.5 wt %, water = 66.3 wt %, 1-decanol = 7.2 wt %—entry D' of Table 1. Similarly, the composition LK = 28.7 wt %, water = 64.6 wt %, 1-decanol = 6.7 wt % at 29 °C—entry C' of Table 1—exhibits a planar texture that is the signature of a ferrocalamitic sample, see Figure 12a.

Both ferronematic structures are sensitive to low-intensity magnetic fields. In refs 14 and 15, a Frederiks transition is reported occurring in a ferrodiscotic capillary cell of thickness  $\sim 100 \mu\text{m}$  under a magnetic field applied parallel to the director of the homeotropic texture. The threshold is of the order of a few kA/m. In Figure 12 we show the field-induced texture transformations in a cell with a planar initial orientation. The images in parts a and b of Figure 12 differ considerably owing to the magnetic field of about 5 kA/m applied parallel to the cell plane.

## 4. Discussion

Our results concerning the location of the nematic domain for the system potassium laurate/1-decanol/water prove, as it was already mentioned by other authors,<sup>16,17</sup> the smallness of this nematic domain (Figure 3) in the composition and temperature scales. In the above-proposed experimental procedure the measures ensuring the absence of lauric acid in our compositions allow us to obtain a lyotropic system with a phase diagram that is well-reproducible and does not depend on the actual set of experiments. This point is especially important since the results by different authors deviate considerably from one another. For example, superimposing of the phase diagrams of the same system presented in refs 16–18 reveals a mismatch of about 1 wt %. Such an uncertainty is substantial since the widths of the concentration domains under discussion range from 0.1 to 1 wt %.



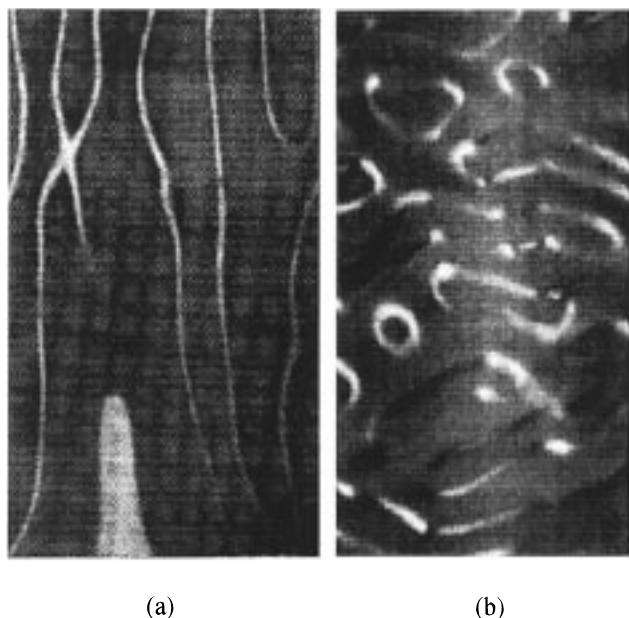


**Figure 12.** Microscopic observation between crossed polarizer and analyzer of a lyotropic composition LK = 28.7 wt %, water = 64.6 wt %, 1-decanol = 6.7 wt % at 29 °C in capillaries of 100  $\mu\text{m}$  thickness: (a) planar configuration, corresponding to a ferrocalamitic sample; (b) same sample but subjected to a constant field of about 60 Oe applied parallel to the cell plane.

Exploring the borders of the nematic region in the undoped system, we identify, along with the isotropic state, several other structure organizations, e.g., a hexagonal-like one. Further investigations are necessary in order to unambiguously correlate the microscopic observations with the sample textures.

Remarkable are the details of the isotropic–nematic transition. At the lowest temperatures, it is clearly of the first-order kind with a distinctive diphasic region. However, at higher temperatures the diphasic domain does not resolve, whereas the pretransitional birefringence fluctuations enhance considerably when approaching the phase transformation threshold.

Ferronematics of either discotic or calamitic structure can be synthesized using magnetic colloids (ferrofluids) with grains in the nanoscopic size range, the same as the micelle size.<sup>18</sup> Surprisingly, to obtain homogeneous ferrolyotropic mixtures stable over several months, it is necessary to use positively charged particles. In water at pH 10, that of the lyotropic matrix, these particles are supposed to reverse their surface charge,<sup>29</sup> because of their acid base behavior. However, pH 10 is not sufficiently alkaline to prevent particles agglomeration especially in the presence of potassium cations, which are known to induce the flocculation of such particles.<sup>29</sup> Despite that, flocculation does not occur in our lyotropic ferrodispersions.

To account for this fact, we assume that as soon as the cationic particles are introduced in the lyotropic mixture, the anionic surfactant (the laurate chain) adsorbs on them. Then, a double layer of surfactant is formed on the particle surface, some molecules of 1-decanol being certainly incorporated into its outer part. Note that, in fact, the number of the suspended particles is very small as compared to the number of surfactant molecules. Because of that, the proposed mechanism does not suppose any noticeable change of the amount of the “free” LK in the mixture. Adsorption of about 1 of 100 molecules of LK is sufficient.

In this model, the doped system appears as a mixture of the usual anisotropic micelles, as in the undoped lyotropic system, with the micelles that have a solid ferrite particle as a core and that should be more spherical because of this core. This concept allows one to explain some of the experimental results we find, for example, the role of the concentration of LK and 1-decanol, which may be related to the adsorption equilibria on particles. However, expulsion of particles from self-organizing surfactants is a phenomenon that is not easy to interpret without osmotic pressure measurements. Further studies (especially small-angle neutrons scattering) are clearly needed to test the validity of our model and to more accurately characterize the diverse states revealed while building up phase diagrams for the magnetically doped lyotropic liquid-crystalline systems.

**Acknowledgment.** Authors are grateful to S. N. Lysenko for helpful discussions and to V. N. Sdobnov for support in performing IR spectroscopy and conoscopic measurements. The work was done under the auspices of the “Le Réseau Formation – Recherche” of MENESRI #96P0079, grant 98-02-16453 of RFBR, and, for V.B., grant 97-06 of the Russian Federal Program “Integration” (Western Urals Division).

## References and Notes

- (1) Ligoure C.; Bouglet G.; Porte G. *Phys. Rev. Lett.* **1993**, *71*, 3600.
- (2) Radlinska E. Z.; Gulik-Krzywicki T.; Lafuma F.; Langevin D.; Urbach W.; Williams C. E.; Ober R. *Phys. Rev. Lett.* **1995**, *74*, 4237.
- (3) Poulin P.; Raghunathan V. A.; Richetti P.; Roux D. *J. Phys. II* **1994**, *4*, 1557.
- (4) Fabre P.; Cassagrande C.; Veyssié M.; Cabuil V.; Massart R. *Phys. Rev. Lett.* **1990**, *64*, 539.
- (5) Bacri J.-C.; Cabuil V.; Cebers A.; Ménager C.; Perzynski R. *Mater. Sci. Eng. C* **1995**, *2*, 197.
- (6) Ménager C.; Belloni L.; Cabuil V.; Dubois E.; Gulik-Krzywicki T.; Zemb Th. *Langmuir* **1996**, *12*, 3516.
- (7) Quilllet C.; Ponsinet V.; Cabuil C. *J. Phys. Chem.* **1994**, *98*, 3566.
- (8) Ott A.; Urbach W.; Langevin D.; Ober R.; Waks M. *Europhys. Lett.* **1990**, *12*, 395.
- (9) de Gennes P. G.; Prost J. *The Physics of the Liquid Crystals*, 2nd ed.; Clarendon: Oxford, 1993.
- (10) Brochard F.; de Gennes P. G. *J. Phys. (France)* **1970**, *31*, 691.
- (11) Burylov S. V.; Raikher Yu. L. *Mol. Cryst. Liquid Cryst.* **1995**, *258*, 107; 123.
- (12) Liebert L.; Martinet A. *J. Phys. Lett. (France)* **1979**, *40*, L-363.
- (13) Figueiredo Neto A. M.; Saba M. M. F. *Phys. Rev. A* **1986**, *34*, 3483.
- (14) Berejnov V.; Raikher Yu.; Cabuil V.; Bacri J.-C.; Perzynski R. *J. Colloid Interface Sci.* **1998**, *199*, 215.
- (15) Berejnov V.; Raikher Yu.; Cabuil V.; Bacri J.-C.; Perzynski R. *Europhys. Lett.* **1998**, *41*, 507.
- (16) Yu L. J.; Saupe A. *Phys. Rev. Lett.* **1980**, *45*, 1000.
- (17) Galerme Y.; Marcerou J. P. *Phys. Rev. Lett.*, **1983**, *51*, 2109.
- (18) Hendrix Y.; Charvolin J.; Rawiso M.; Liebert L.; Holms M. C. *J. Phys. Chem.* **1983**, *87*, 3991.
- (19) Nakanishi K. *Infrared Absorption Spectroscopy*; Nancodo: Tokyo, 1965.
- (20) Berejnov V. Thesis, Université Pierre et Marie Curie, Paris, 1998.
- (21) Hartshorne N. H.; Stuart A. *Crystals and the Polarising Microscope*, 4th ed.; Edward Arnold: London, 1968.
- (22) Massart R. *IEEE Trans. Magn.* **1981**, *17*, 1247.
- (23) Bacri J.-C.; Perzynski R.; Salin D.; Cabuil V.; Massart R. *J. Magn. Mater.* **1986**, *62*, 36.
- (24) Sonin A. S. *Sov. Phys. Usp.* **1987**, *30*, 875.
- (25) Oswald P.; Kleman M. *J. Phys. (France)* **1981**, *42*, 1461.
- (26) Ramos L. Thesis, Université Pierre et Marie Curie, 1997.
- (27) Hendrix Y.; Charvolin J. *J. Phys. (France)* **1981**, *41*, 1427.
- (28) Berejnov V.; Dubois E.; Boué F.; Cabuil V.; Perzynski R.; Raikher Yu. Unpublished results.
- (29) Bacri J.-C.; Perzynski R.; Salin D.; Cabuil V.; Massart R. *J. Magn. Mater.* **1990**, *85*, 27.